

Distribution of electric potential at the surface of corona-charged polypropylene non-woven fabrics after neutralization

Belkacem Yahiaoui,
Mohamed Magharbi,
Belaid Tabti
University A.Mira
Bejaia, Algeria
Bel.yahiaoui@yahoo.com

Angela Antoniu,
Senior Member, IEEE
Atallah Smaili
Institut P', UPR3346, CNRS
University of Poitiers-ENSMA
IUT, 16021 Angoulême, France

Lucian Dascalescu
Fellow, IEEE
Institut P', UPR3346, CNRS
University of Poitiers-ENSMA
IUT, 16021 Angoulême, France
lucian.dascalescu@univ-poitiers.fr

Abstract – Accumulation of electric charges on insulating surfaces is frequently at the origin of severe electrostatic hazards. The best solution to this problem is to neutralize these charges by the use of AC corona discharges. The aim of this work is to evaluate the efficiency of this process in the specific case of fibrous electrets, by measuring the repartition of the electric potential at the surface of non-woven polypropylene (PP) fabrics before and after neutralization. The samples were charged for 10 s, in ambient air, using a triode-type corona electrode system of positive polarity. In all the experiments, the neutralization was performed 180 s after the charging process. In some of them, the neutralization electrode (tungsten wire, diameter: 0.3 mm) was fixed at a given distance (50 mm) above the samples and energized from an AC voltage amplifier (model 30/20A, Trek Inc. Medina, NY). In other experiments, the samples moved at constant speed (3 cm/s) in the AC corona discharge zone generated by the neutralization electrode. The experimental results show that the efficiency of neutralization (expressed as the relative reduction of the average potential measured at the surface of the sample) depends on the amplitude and the frequency of the sinusoidal high-voltage, as well as on the charging time and the neutralization duration. Better effects were recorded in the case of the samples that moved through the corona discharge zone.

Index Terms— surface potential distribution, corona discharge, charge neutralization, fibrous electrets

I. INTRODUCTION

The accumulation of electric charge on the surface of insulating materials may enhance the collection efficiency of the air filters that use polypropylene (PP), polycarbonate (PC), polyethylene (PE) and other fibrous polymers with extremely low electrical conductivity [1-7]. Corona discharge is the most frequently used method for the electric charging of the filtration media. Metal wires energized from DC high-voltage supplies commonly serve as corona electrodes [8]. The using of the triode-type electrode arrangements can be employed to generate a uniform discharge and better control the potential at the sample surface [9]. In some cases, the electric charge accumulates on the media at different place on the production line, due to tribo-charging effects inherent to material handling [10] and this phenomenon can be harmful to either the operator or to the electronic device.

The electrostatic discharges cause to industry considerable losses [11-13], in spite of the fact that there are various ways to control static electricity [14-16]. "Passive" neutralization is based on the ionization of the air in the proximity of conductive points or sharp edges of small curvature radius, connected to the ground [17, 18]. The efficiency of this method is rather low, as compared with the "active" neutralization, which make use of custom-designed ionizers [19]. These devices, which are typically energized from AC high-voltage supplies, produce both positive and negative ions to be attracted by the charged surface so that neutralization can occur.

In two recent papers [20, 21], the authors have addressed the problem of the accelerated discharge of fibrous dielectrics. They pointed out that the neutralization achieved with a commercial ion generator depends on the nature of the processed materials, the distance between the neutralizer and the substrate, the duration of exposure and the position of the sample with respect to the grounded electrode. Then, they evaluated two of the factors that influence the charge elimination on non-woven PP and PE fabrics: the frequency and the amplitude of sinusoidal or triangular high-voltage neutralizers. In both above-cited papers, the charging state of the non-woven fabrics was evaluated by electric potential measurements [22-24] performed in one point at the surface of the sample.

The record of potential repartition at the surface of the sample [25] is likely to provide more information on the charging state of the media and enable the refinement of the previous studies on the neutralization of corona-charged non-woven fabrics. The present work takes advantage of this technique and aims at a more accurately evaluation of the efficiency of two methods of charge neutralization (stationary and in-motion), for the particular case of PP non-woven fabrics. The neutralization rate (i.e., the relative reduction of the average potential at the surface of the samples) is determined under various experimental conditions, the factors under study being the frequency and the amplitude of the sinusoidal high-voltage that energizes the neutralizer, the duration of charging, and the duration of the exposure to the AC corona discharge.

II. MATERIALS AND METHODS

The experiments were performed on 120 mm x 90 mm samples cut from the same non-woven polypropylene fabric (sheet thickness: 400 μm ; fiber diameter: 28 μm), in ambient air (temperature: 15°C to 19°C; relative humidity: 40% to 48%). The samples were placed on an aluminium plate (165 mm x 115 mm) connected to the ground. The electric charging of the samples was performed using a triode electrode system (Fig. 1) that consists of a high-voltage wire-type dual electrode [26], facing the grounded plate electrode and a grid electrode (Fig. 2). The high-voltage electrode consists of a tungsten wire (diameter 0.3 mm) suspended by a metallic cylinder (diameter 26 mm) at 34 mm distance from the axis. The grid is located at equal distance from the corona wire and the surface of the plate electrode. The wire and the cylinder were energized from the same adjustable high-voltage supply, 100 kV, 3 mA (model SL300 Spellman, Hauppauge, NY), as shown in Fig. 3.

The grid is connected to the ground through a series of calibrated resistors of a total resistance R . In this way, for a current intensity I , a well-defined potential $V_g = RI$ is imposed between the grid and the grounded plate on which the samples are deposited. Parts of the ions generated by the corona electrode pass through the grid and are driven by this potential to the surface of the media, which retains them. The potential at the surface of the media V_{surf} is limited by the potential of the grid V_g or by the partial discharge voltage of the sample V_b . In all the experiments described hereafter $V_g = 3 \text{ kV}$.

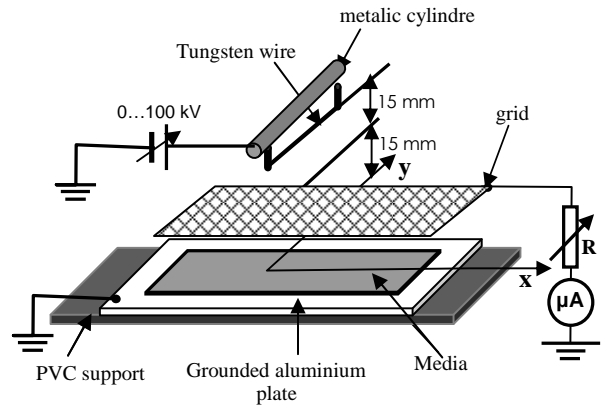


Fig. 1. Wire –grid –plane electrode charging system.

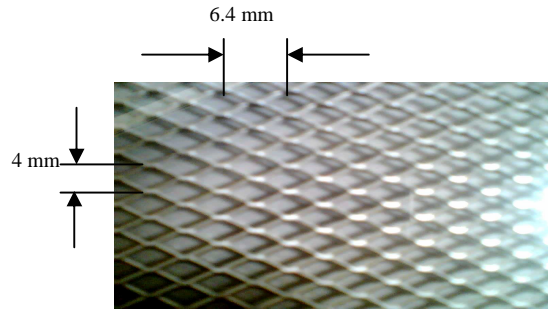


Fig. 2. Metallic grid,

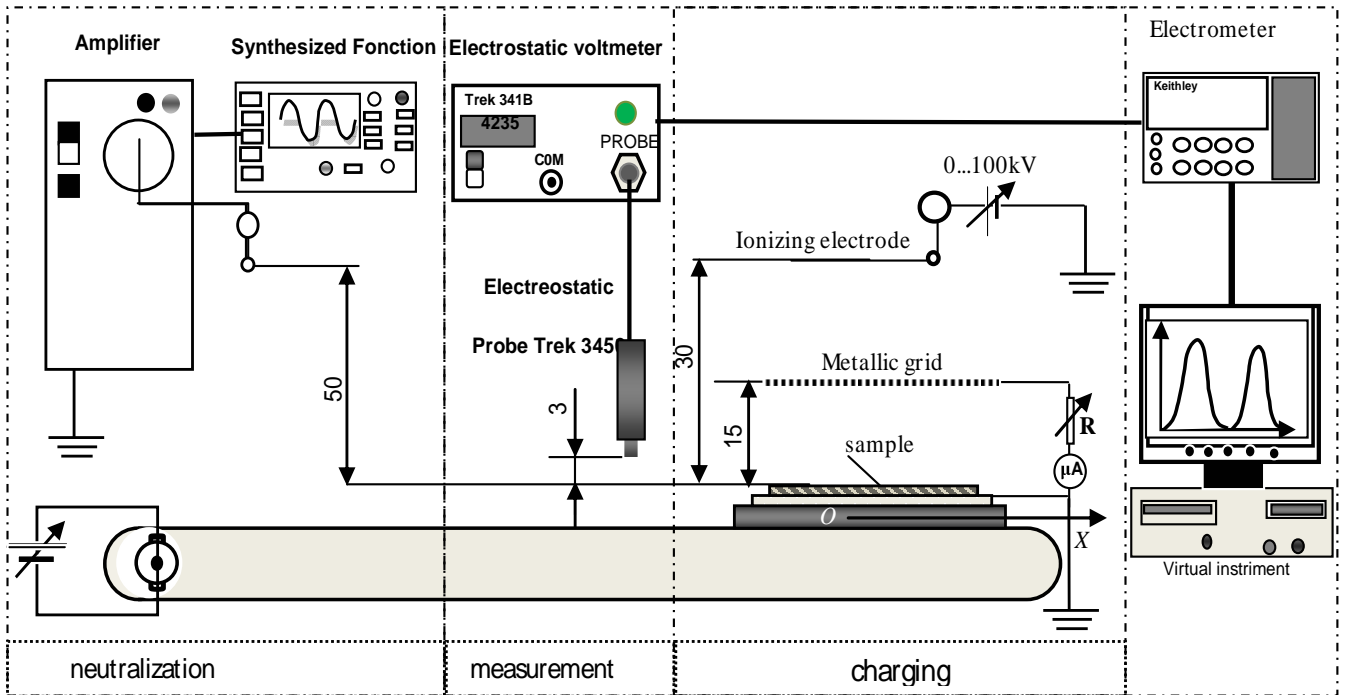


Fig. 3. Experimental set-up for the measurement of the surface potential before and after neutralization

The sample carrier consisted of a PVC plate, to which the assembly plate electrode + non-woven fabric was firmly attached. A conveyor belt supported the sample carrier and transferred it from the charging position to the surface potential measurement and charge neutralization sections of the experimental set-up. The speed of the conveyor could be adjusted from 1 cm/s to 6 cm/s, for the various needs of the experiments.

As soon as the high-voltage supply of the corona charger was turned-off, the conveyor belt transferred the samples at a constant speed through the measurement section. Thus the repartition of the surface potential along the central axis Ox of the sample was measured with an electrostatic voltmeter (model 341B), equipped with an electrostatic probe (model 3450, Trek Inc., Medina, NY), and recorded via an electrometer (model 6514, Keithley Instruments, Cleveland), connected to a personal computer. The acquisition and processing of experimental data was performed using an ad-hoc virtual instrument, developed in LabView environment.

The neutralization was performed with a dual wire-type electrode similar to the one described above, connected to a high-voltage amplifier 30 kV, 20 mA (model 30/20A, Trek Inc., Medina, NY). The amplitude U_n and the frequency f of the high-voltage were adjusted using a synthesized function generator (model FG300, Yokogawa, Japan). The neutralizer – sample spacing was 50 mm (Fig. 3). The potential at the surface of the sample after neutralization was measured using the previously-described method.

In the three series of experiments described in this paper the surface potential was measured at various instants t_i after charging the samples and once again at $t_2 = 30$ s after neutralization. The N rate was expressed in function of V_1 and V_2 , which were the mean values of the potential along the central axis Ox of the sample respectively before and after neutralization:

$$N [\%] = [1 - (V_2/V_1)] \times 100 \quad (1)$$

In a preliminary experiment the samples were charged for $T_c = 30, 10$ and 2 s, and the repartition of the surface potential was recorded at $t_i = 30, 90, 180, 600$ and 900 s.

For the first and second set of experiments, the charging duration was maintained constant at respectively $T_c = 10$ s, and $T_c = 2$ s, with the neutralization time fixed at either $T_n = 2$ s or $T_n = 4$ s. The amplitude of the neutralization voltage was varied at three levels: $U_n = 16, 20$ and 24 kV. The voltage frequency was adjusted to four values $f = 50, 100, 200, 400$ Hz. For each combination (U_n, f) , the tests were repeated three times, and each run was performed on a new sample.

The third sets of experiments were carried out at constant charging duration $T_c = 10$ s, but the neutralization was performed with the sample moving at a constant speed (3 cm/s) through the AC corona discharge zone, so that the sample passage from end to end under the neutralizer to last roughly 4 s. In this way, the durations of the “in-motion” and some of the “stationary” neutralization were similar.

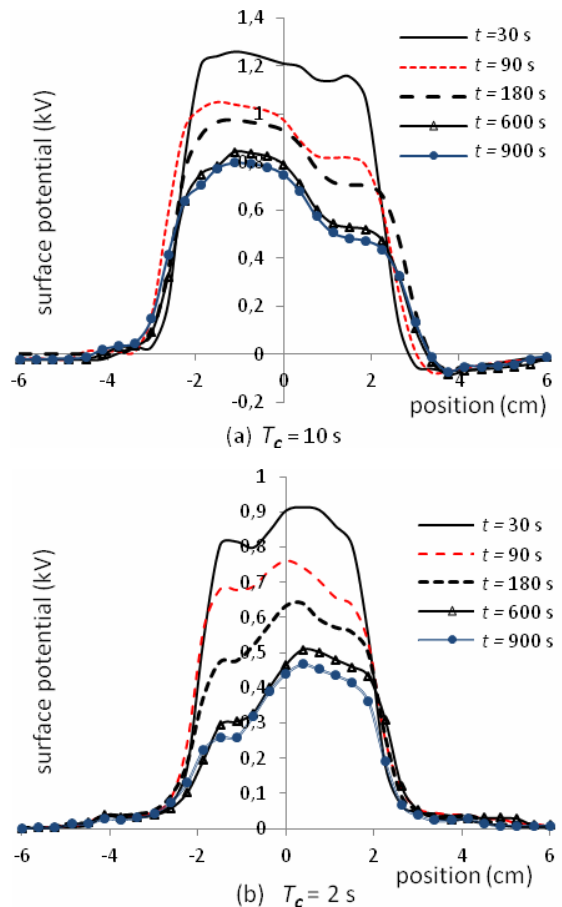


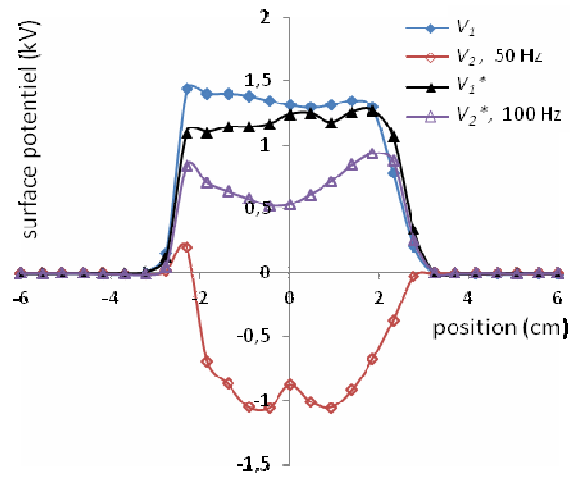
Fig. 4. Repartition of the surface potential along the Ox axis for PP sample in contact with the grounded electrode, at various instants t , for two values of the charging time (a) $T_c = 10$ s, (b) $T_c = 2$ s (grid potential $V_g = 3$ kV).

III. RESULTS AND DISCUSSION

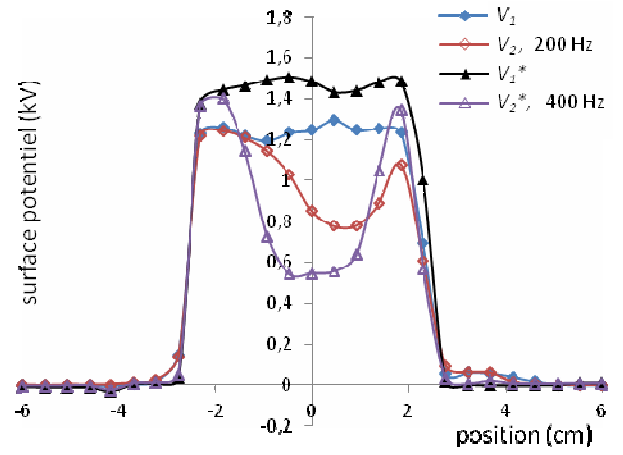
The preliminary set of experiments pointed out the surface potential decay during the first 900 s = 15 min after corona-charging (Fig. 4). This decay is due to the combined action of several physical mechanisms (partial discharges, recombination, and lateral and transversal conduction), and is known to be influenced by the value of the charging potential [23, 27]. The initial potential is higher and roughly the same in the case of the two longer charging duration $T_c = 30$ and 10 s. This means that shorter charging duration $T_c = 2$ s is not enough to charge the sample at saturation. However, in all the cases, the charge decay after 180 s was slow enough to consider that it did not affect the accuracy of the surface potential repartition measurements.

A. Effects of AC voltage amplitude and frequency

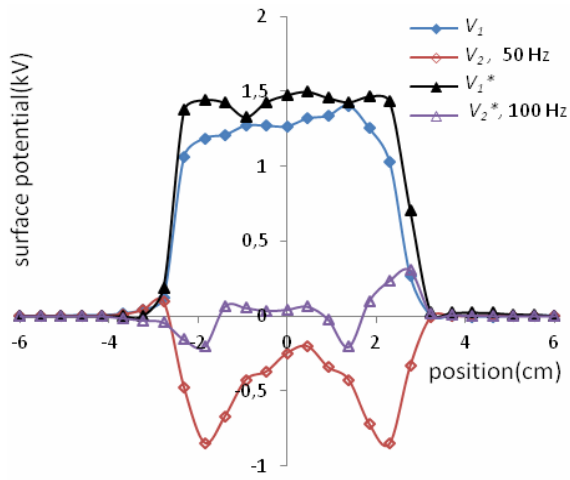
Figs. 5 and 6 present typical surface potential repartition profiles obtained under various AC corona neutralization conditions. The non-uniformity of these profiles before neutralization is due to the non homogeneous structure of the media [25]. The average surface potential after charging is in the range 1.25 – 1.5 kV.



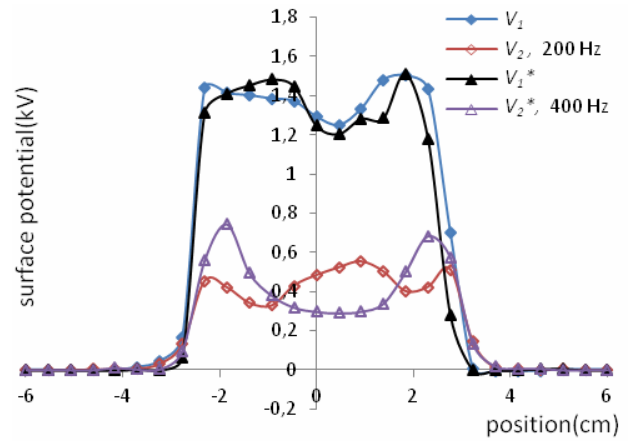
(a) $U_n = 16 \text{ kV}, T_c = 10 \text{ s}, T_n = 2 \text{ s}$



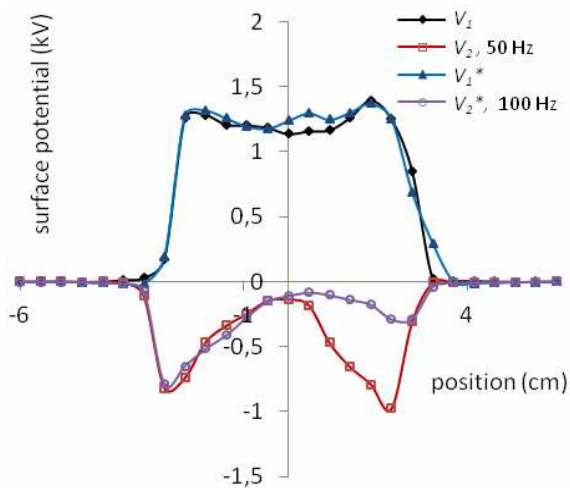
(b) $U_n = 16 \text{ kV}, T_c = 10 \text{ s}, T_n = 2 \text{ s}$



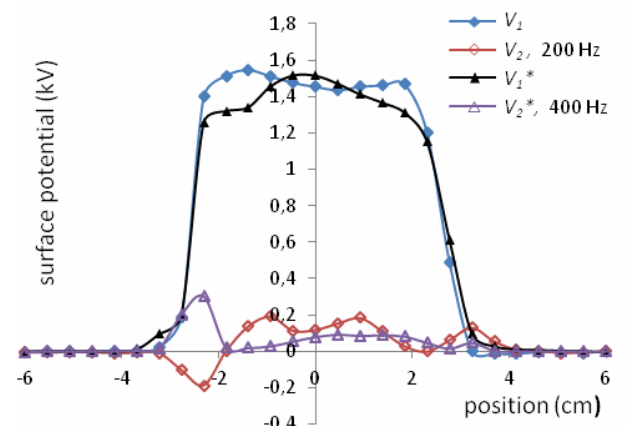
(c) $U_n = 20 \text{ kV}, T_c = 10 \text{ s}, T_n = 2 \text{ s}$



(d) $U_n = 20 \text{ kV}, T_c = 10 \text{ s}, T_n = 2 \text{ s}$

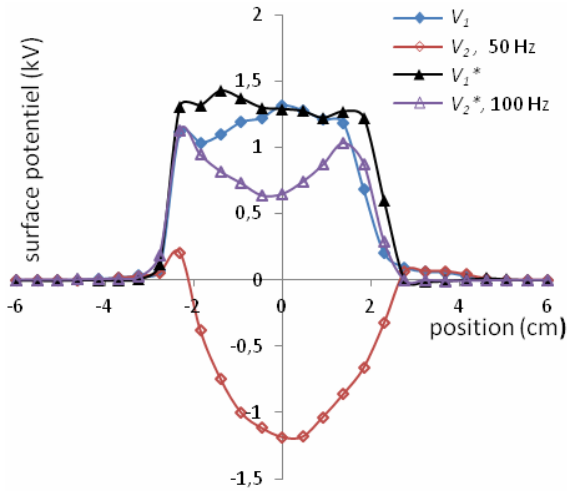


(e) $U_n = 24 \text{ kV}, T_c = 10 \text{ s}, T_n = 2 \text{ s}$

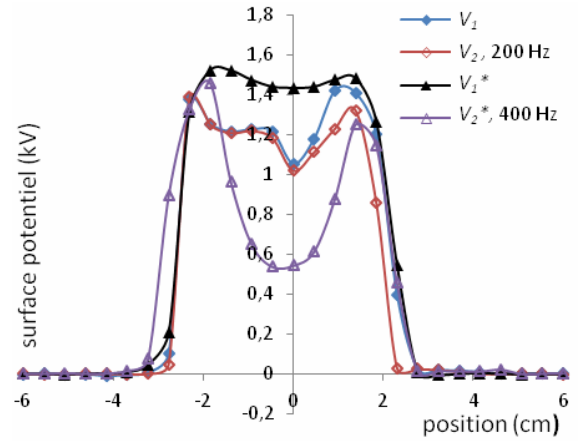


(f) $U_n = 24 \text{ kV}, T_c = 10 \text{ s}, T_n = 2 \text{ s}$

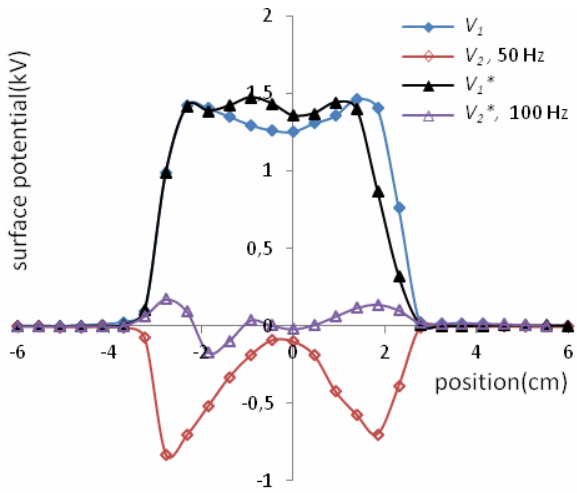
Fig. 5. Typical curves of the surface potential distribution before V_1 and after neutralization V_2 , charging duration $T_c = 10 \text{ s}$. The neutralization was performed 3 min after corona-charging turn-off, during $T_n = 2 \text{ s}$, using a sinusoidal high-voltage with various amplitudes and frequencies.



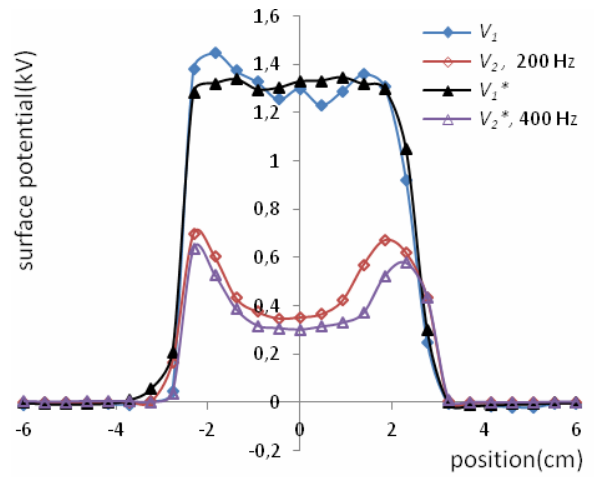
(a) $U_n = 16 \text{ kV}, T_c = 10 \text{ s}, T_n = 4 \text{ s}$



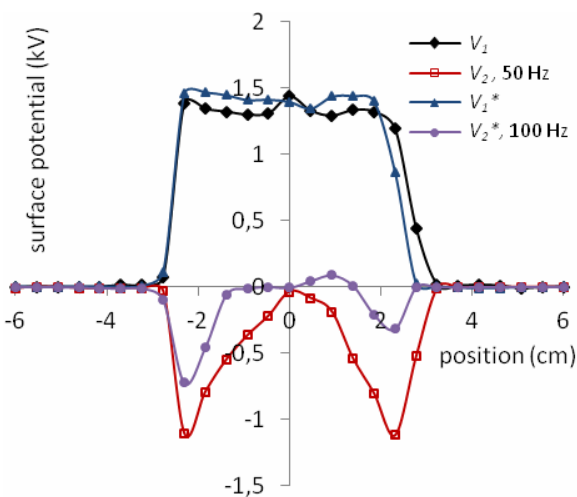
(b) $U_n = 16 \text{ kV}, T_c = 10 \text{ s}, T_n = 4 \text{ s}$



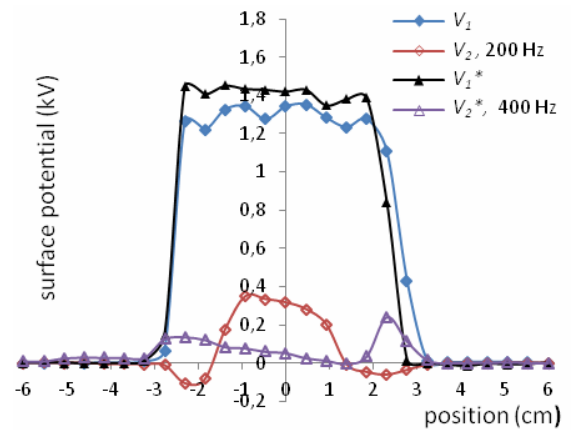
(c) $U_n = 20 \text{ kV}, T_c = 10 \text{ s}, T_n = 4 \text{ s}$



(d) $U_n = 20 \text{ kV}, T_c = 10 \text{ s}, T_n = 4 \text{ s}$



(e) $U_n = 24 \text{ kV}, T_c = 10 \text{ s}, T_n = 4 \text{ s}$



(f) $U_n = 24 \text{ kV}, T_c = 10 \text{ s}, T_n = 4 \text{ s}$

Fig. 6. Typical curves of the surface potential distribution before V_1 and after neutralization V_2 , charging duration $T_c = 10 \text{ s}$. The neutralization was performed 3 min after corona-charging turn-off, during $T_n = 4 \text{ s}$, using a sinusoidal high-voltage with various amplitudes and frequencies.

The surface potential repartition after neutralization is not symmetrical (Figs. 5.b, e) because of the imperfections of the experimental set-up: the wire neutralizer cannot be precisely positioned on the axis of the sample. However, when the axes of the wire and of the sample are in the same vertical plane, the repartition of the surface potential after neutralization is symmetrical, and the maximum effect is obtained in the middle of the sample, as in Fig. 6.d.

The surface potential repartition after neutralization is directly related to the frequency and the amplitude of the neutralization voltage. For the frequency $f = 50$ Hz, and all amplitude levels, the surface potential after neutralization is negative, i.e. of opposite polarity to the initial potential, as shown in Figs. 5.a, c, e, and 6.a, c, e). This means that the initial charges are completely neutralized and new charges are deposited at the surface of the samples. At a higher frequency $f = 100$ Hz, the degree of neutralization depends on the amplitude of the sinusoidal high voltage applied to the corona electrode. Thus, the neutralization is almost total for $U_n = 20$ kV, but negative charges are deposited by the AC corona discharge at $U_n = 24$ kV. In the experiments carried out at $f = 200$ and 400 Hz, the neutralization is more effective at higher amplitudes of the applied AC high-voltage (Figs. 5.b, d, f, and 6.b, d, f). These observations can be straightforwardly explained by the lower corona onset voltage at negative polarity and the higher mobility of the negative ions generated by the AC corona ionizer.

The variation of the ratio V_2/V_1 as a function of the frequency f for three amplitudes $U_n = 16, 20$ and 24 kV of the neutralisation voltage is shown in Fig. 7. In all cases this ratio is negative at $f = 50$ Hz. For $U_n = 24$ kV, it remains negative at $f = 100$ Hz, but is positive at the other frequencies. The change of sign of the ratio V_2/V_1 means that for each voltage level U_n there is a frequency f_0 where the neutralization is complete. Thus, $f_0 = 65, 85$ and 150 Hz, for $U_n = 16, 20$ and 24 kV, respectively.

B. Effect of the neutralization duration

The calculated values of the neutralization rate N for two charging durations $T_c = 2$ and 10 s are given respectively in Tables 1 and 2, for the two neutralization durations considered in the present study: $T_n = 2$ and 4 s. The effect of T_n on the neutralization rate N is statistically significant at lower voltage amplitudes U_n and frequencies f , as it can also be observed by examining the curves in Fig. 7. Indeed, exposing the charged samples for a longer time to the AC corona discharge increases the chances of the residual charges to be neutralized by the incoming flux of bipolar ions. However, at higher U_n and/or f , the increase of the neutralization duration is not accompanied by a significant improvement of the neutralization efficiency. A complete explanation of the observed phenomena requires the development of a physical model capable to take into account not only the generation of the bipolar charge and the ion drift to the sample, but also the charge injection and conduction at the surface and in the bulk of the samples.

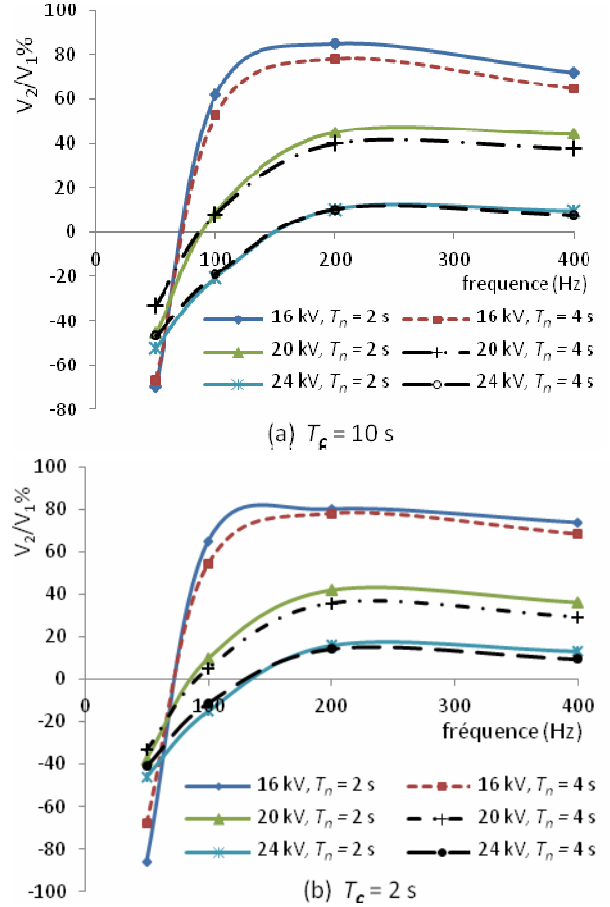


Fig. 7. Variation of the surface potential ratio V_2/V_1*100 as a function of the frequency f of the neutralizing voltage, for $U_n = 16, 20$ and 24 kV, for two neutralization durations (a) $T_n = 2$ s, (b) $T_n = 4$ s.

TABLE I
NEUTRALIZATION RATE $N\%$ AT VARIOUS FREQUENCIES f , AMPLITUDES U_n , AND DURATIONS T_n OF THE NEUTRALIZATION VOLTAGE (CHARGING DURATION $T_c = 10$ s)

f (Hz)	N [%]					
	$U_n = 16$ kV		20 kV		24 kV	
	$t_n = 2$ s	4 s	2 s	4 s	2 s	4 s
50	30.76	33.57	54.53	67.17	48.03	53.53
100	38.2	47.2	90.90	91.85	79.39	80.94
200	15.16	21.69	54.68	60.05	89.45	89.54
400	28.04	35.26	55.58	62.28	90.30	92.12

TABLE II
NEUTRALIZATION RATE $N\%$ AT VARIOUS FREQUENCIES f , AMPLITUDES U_n , AND DURATIONS T_n OF THE NEUTRALIZATION VOLTAGE (CHARGING DURATION $T_c = 2$ s)

f (Hz)	N [%]					
	$U_n = 16$ kV		20 kV		24 kV	
	$t_n = 2$ s	4 s	2 s	4 s	2 s	4 s
50	13.75	31.94	62.28	66.59	53.03	59.06
100	35.22	45.66	90.49	94.96	84.88	88.80
200	20.13	21.98	58.84	63.32	84.08	85.75
400	26.44	31.65	64.04	70.86	86.89	90.59

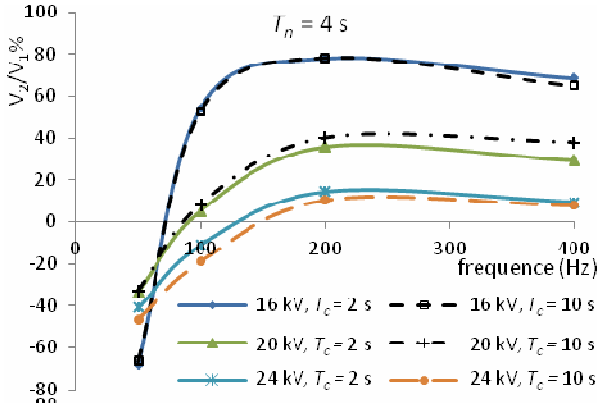


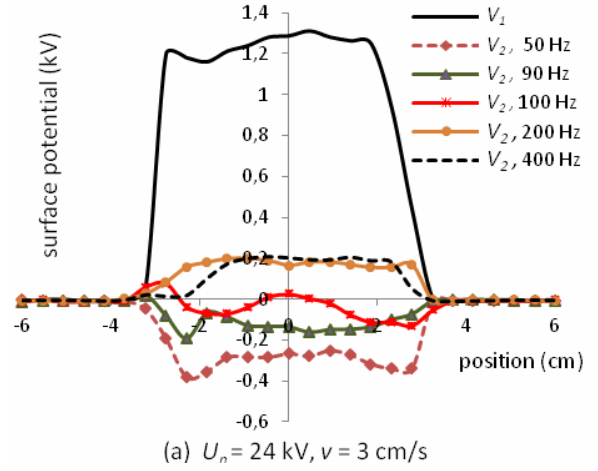
Fig. 8. Variation of the surface potential ratio V_2/V_1*100 as a function of the frequency f of the neutralizing voltage, for $U_n = 16, 20$ and 24 kV, $T_n = 4$ s, for two charging durations $T_c = 2$ and 4 s.

C. Effect of the charging duration

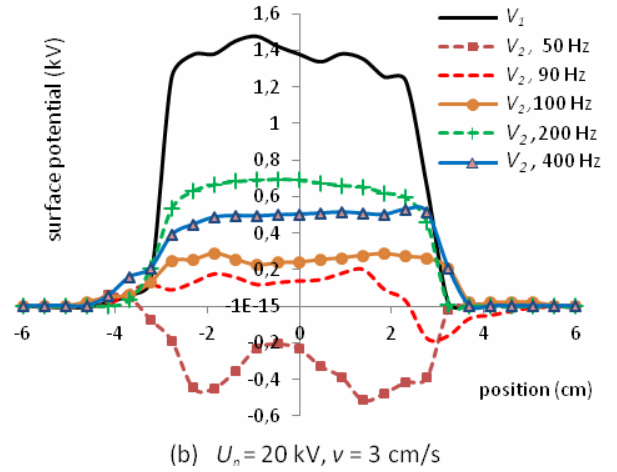
The results of the first and the second experiments carried out at two different charging durations $T_c = 10$ and $T_c = 2$ s are given respectively in Tables I and II. As expected, the neutralization rate was lower in the first case. Indeed, in previous paper [25], the authors have pointed out that the level of the surface potential and the extension of corona-charged area increased with the charging duration. In the case of a longer exposure to the corona discharge, the charges can accumulate not only at the surface of the media but also in the depth of the samples, which have a porous structure. The presence of this charge tends to repel the in-coming ions to the not-yet charged area at the surface of the sample. Thus, a more-and-more larger area of the sample becomes affected by the corona discharge, as it can be also seen in Fig. 4. As a consequence, in order to have the same neutralization rate, more time is needed to neutralize the charges on the surface and in depth of the sample. By examining the results in Tables I and II, this effect can be clearly seen at high frequencies for $U_n = 20$ kV and at low frequencies for the voltage $U_n = 24$ kV, but is less noticeable at $U_n = 16$ kV (Fig. 8). A larger volume of experimental data would be necessary in order to formulate a more firm conclusion on this issue.

D. In-motion neutralization

The results of the third set of experiments, performed with the sample moving through the AC corona discharge zone, are given in Fig. 9. As for the stationary neutralization, the efficiency of the process is correlated to both the amplitude U_n and the frequency f of the high-voltage. For $U = 20$ and 24 kV, the best results were obtained respectively for $f = 90$ and 150 Hz (Fig. 10), similar to the stationary case (see section III, A). The advantage of having the sample in-motion through the AC corona discharge: the repartition of the surface voltage after neutralization is more uniform than in the stationary situation.



(a) $U_n = 24$ kV, $v = 3$ cm/s



(b) $U_n = 20$ kV, $v = 3$ cm/s

Fig. 9. Repartition of the surface potential before (V_1) and after (V_2) neutralization at various frequencies f of the neutralization voltage of amplitude (a) $U_n = 24$ kV and (b) $U_n = 20$ kV.

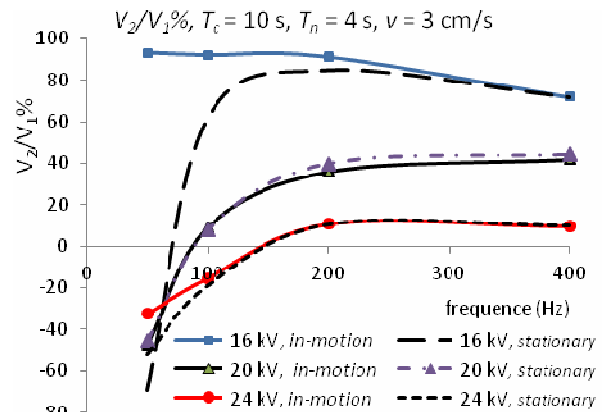


Fig. 10.. Variation of the surface potential ratio V_2/V_1*100 as a function of the frequency f of the AC voltage of amplitude $U_n = 16, 20$ and 24 kV, for the stationary ($T_n = 4$ s) and in-motion (sample speed : 3 cm/s) neutralisation charging durations ($T_c = 4$ s).

IV. CONCLUSIONS

The study of the potential repartition at the surface of the PP samples enabled a better evaluation of the factors that might accelerate the charge neutralization when using the bipolar charge generated in an AC corona discharge.

(1) The efficiency of the process is correlated to both the frequency and the amplitude of the sinusoidal high-voltage applied to the neutralizing electrode. For a non-woven fabric charged under given conditions, at any given amplitude of the applied high-voltage, complete neutralization can be achieved by an appropriate adjustment of the frequency.

(2) The neutralization rate achieved under well-defined conditions (amplitude and frequency of the neutralization voltage, duration of exposure to the AC corona discharge) depends on the charging duration. The longer is the charging duration, the more demanding is the neutralization process.

(3) In the conditions of the experiments described in the present paper, the increase of the neutralization duration improves the efficiency of the process, at lower values of AC high-voltage amplitude and frequency.

(4) In-motion neutralization is at least as effective as the stationary one. This technique is easier to implement in an industrial application.

REFERENCES

- [1] J. van Turnhout, W. J. Hoeneveld, J. W.C. Adamse and L. M. van Rossen, "Electret filters for high efficiency and high flow air cleaning," *IEEE Trans. Ind. Appl.*, vol 17, no. 2, pp. 240–248, 1981.
- [2] R. C. Brown, *Air filtration—An Integrated Approach to the Theory and Applications of Fibrous Filters*, Oxford: Pergamon Press, 1993.
- [3] F. J. Romay, B. Y. H. Liu and S. J. Chae, "Experimental study of electrostatic capture mechanisms in commercial electret filters", *Aerosol Sci. & Technol.*, vol. 28, pp. 224–234, 1998.
- [4] M. Nifuku, Y. Zhou, A. Kisiel, T. Kobayashi, and H. Katoh, "Charging characteristics for electret filter materials", *J. Electrostat.*, vol. 51-52, pp. 200-205, 2001.
- [5] R. Kacprzyk, "Non-conventional application of unwoven fabrics," *J. Electrostat.*, vol. 56, pp. 111-119, 2002.
- [6] D. L. Myers and B. D. Arnold, "Electret media for HVAC filtration applications," *INJ Winter*, 2003, pp. 43-54.
- [7] I. M. Hutten, *Handbook of Nonwoven Filter Media*. Oxford: Elsevier, 2007.
- [8] B. Tabti, M. Mekideche, M. Plopeanu, L.M. Dumitran, L. Herous, and L. Dascalescu, "Corona charging and charge decay characteristics of non-woven filter media," *IEEE Trans. Ind. Appl.*, vol. 46, no. 2, pp.634–640, 2010.
- [9] T. Oda and J. Ochiai, "Charging characteristics of a non- woven sheet air filter," *Proc. 6th Int. Symp. on Electrets*, 1981, pp. 515-518.
- [10] P.A. Smith, G.C. East, R.C. Brown and D. Wake, "Generation of triboelectric charge in textile fibre mixtures and their use as air filters", *J. Electrostat.*, vol. 21, pp. 81-98, 1988.
- [11] C. Duvvury and E. A. Amerasekera, *ESD in Silicon Integrated Circuits*, New York, NY, USA: Wiley, 2002.
- [12] W. D. Greason, *Electrostatic Discharge in Electronics*, New York, NY, USA: Wiley, Research Studies Press, 1992
- [13] S. H. Voldman, "The state of the art of electrostatic discharge protection: physics, technology, circuits, design, simulation, and scaling", *IEEE J. Solid State*, vol. 34, no. 9, pp. 1272-1282, 1999.
- [14] I. Alexeff, and W.L. Kang, "An enhanced ionizer," *IEEE Trans. Plasma Sci.*, Vol. 27 , no. 1, pp. 32-33, 1999.
- [15] J.-S. Chang, "Neutralization theory of static surface charge by an ionizer under wide gas pressure environments," *IEEE Trans Ind Appl.*, vol. 37, no. 6, pp. 1641-1645, 2001.
- [16] D. Callinan, "Combating static charges from plastic components," *Converters*, vol. 42, no. 12, pp. 16-17, 2005
- [17] T. Horvath and I. Berta, *Static Elimination*, New York, NY, USA: Wiley, Research Studies Press, 1982.
- [18] K. Robinson, "Choosing passive or active ionizers", *Paper, Film and Foil Converter*, vol. 84, no. 7 pp. 10, 2010.
- [19] Y. Tabata, T. Kodama, W. L. Cheung, and N. Nomura, "General characteristics of a newly developed bipolar static charge eliminator," *J. Electrostat.*, vol. 42, pp. 193-202, 1997.
- [20] A. Antoniu, B. Tabti, M. C. Plopeanu, and L. Dascalescu, "Accelerated discharge of corona-charged non-woven fabrics," *IEEE Trans. Ind. Appl.*, vol. 46, no. 3, pp. 1188-1193, 2010.
- [21] A. Antoniu, A. Smaili, I-V. Vacar, M. C. Plopeanu and L. Dascalescu, "Sinusoidal and triangular AC high-voltage neutralizers for accelerated discharge of non woven fibrous dielectrics" *IEEE Trans. Ind. Appl.*, vol. 48, 2012 (in press).
- [22] D. M. Taylor, and P. E. Secker, *Industrial Electrostatics: Fundamentals and measurements*, New York, NY, USA: Wiley, Research Studies Press, 1994.
- [23] P. Molinié and P. Llovera, "Surface potential measurements: Implementation and interpretation," *Diel. Mater. Meas. Appl., IEEE Conf Publ. No. 473*, 2000, pp. 253–258.
- [24] M. A. Noras, "Non-contact surface charge/voltage measurements. capacitive probe-principle of operation", *Trek Application Note, number 3001*, pp. 1 –8, 2002.
- [25] M-C. Plopeanu, L. Dascalescu, B. Yahiaoui, A. Antoniu, M. Hulea, and P. V. Notingher " Repartition of electric potential at the surface of non-woven fabrics for air filtration" *IEEE Trans. Ind. Appl.*, vol. 48, 2012 (in press).
- [26] L. Dascalescu, A. Iuga, R. Morar, V. Neamtu, I. Suarasan, A. Samuila, and D. Rafiroiu., "Corona and electrostatic electrodes for high-tension separators," *J. Electrostat.*, vol. 29, pp. 211-225, 1993.
- [27] B. Tabti, M. Mekideche, M. C. Plopeanu, L. M. Dumitran, A. Antoniu, and L. Dascalescu, "Factors that influence the decay rate of the potential at the surface of non woven fabrics after negative corona discharge deposition," *IEEE Trans. Ind. Appl.*, vol. 46, no. 4, pp. 1586–1592, 2010.